frontiers in Materials

ORIGINAL RESEARCH
published: 12 January 2022
doi: 10.3389/fmats.2021.810535

Effect of Aluminum Incorporation on the Reaction Process and Reaction Products of Hydrated Magnesium Silicate

Yuan Jia[1,2], Yuxin Zou[2], Xinmei Zou[2], Yaoting Jiang[2], Fangyuan Li[2], Wangkun Ma[3], Hongli Yan[4] and Rui Hua[4]*

[1]Hebei Provincial Laboratory of Inorganic Nonmetallic Materials and Hebei Provincial Industrial Solid Waste Comprehensive Utilization Technology Innovation Center, Tangshan, China, [2]College of Materials Science and Engineering, North China University of Science and Technology, Tangshan, China, [3]Technical Information Research Institute of Building Materials Industry, Beijing, China, [4]China Railway 14th Bureau Group 2nd Engineering Co., Ltd., Taian, China

In this study, we investigated the impact of aluminium ion (Al^{3+}) incorporation on the microstructure and the phase transformation of the magnesium silicate hydrate system. The magnesium silicate hydrate system with aluminium was prepared by mixing magnesium oxide and silica fume with different aluminium ion contents (the Al/Si molar ratios of 0.01, 0.02, 0.05, 0.1, 0.2) at room temperature. The high degree of polymerization of the magnesium silicate hydrate phases resulted in the limited incorporation of aluminium in the structure of magnesium silicate hydrate. The silicon-oxygen tetrahedra sites of magnesium silicate hydrate layers, however, were unable to substitute for silicon sites through inverted silicon-oxygen linkages. The increase in aluminium ion content raised the degree of polymerization of the magnesium silicate hydrate phases from 0.84 to 0.92. A solid solution was formed from residual aluminum-amorphous phases such as hydroxyl-aluminum and magnesium silicate hydrate phases. X-ray diffraction (XRD), field emission scanning electron microscope (F-SEM), and ^{29}Si and ^{27}Al MAS NMR data showed that the addition of Al^{3+} promotes the hydration process of MgO and has an obvious effect on the appearance of M-S-H gel. The gel with low aluminum content is fluffy, while the gel with high aluminum content has irregular flakes. The amount of Al^{3+} that enters the M-S-H gel increased with the increase of Al^{3+} content, but there was a threshold: the highest Al/Si molar ratio of M-S-H gel can be maintained at about 0.006.

Keywords: magnesium silicate hydrate system, hydroxyl-aluminum, phase transformation, microstructure, aluminium ion content

OPEN ACCESS

Edited by:
Lijie Guo,
Beijing General Research Institute of Mining and Metallurgy, China

Reviewed by:
Zhihong Zhang,
Beijing University of Technology, China
Daiqiang Deng,
Xiangtan University, China

****Correspondence:***
Yuan Jia
jia132012@ncst.edu.cn

Specialty section:
This article was submitted to Structural Materials, a section of the journal Frontiers in Materials

Received: *07 November 2021*
Accepted: *08 December 2021*
Published: *12 January 2022*

Citation:
Jia Y, Zou Y, Zou X, Jiang Y, Li F, Ma W, Yan H and Hua R (2022) Effect of Aluminum Incorporation on the Reaction Process and Reaction Products of Hydrated Magnesium Silicate. Front. Mater. 8:810535. doi: 10.3389/fmats.2021.810535

INTRODUCTION

As we all know, the hydration product of $CaO\text{-}SiO_2\text{-}H_2O$ system is calcium silicate hydrate (C-S-H) gel, like C-S-H, at normal temperatures and pressures, and the main hydration product of $MgO\text{-}SiO_2\text{-}H_2O$ system is magnesium silicate hydrate (M-S-H)gel(Li et al., 2014; Jia et al., 2017a). The molecular structures of magnesium silicate hydrate (M-S-H) and calcium silicate hydrate (C-S-H) phases are significantly different. The former is an amorphous precursor of talc or sepiolite with layered silica structure (Lothenbach et al., 2015; Bernard et al., 2019), while the latter is a silica-deficient solid solution and is a precursor of two crystalline phases, tobernorite and jennite

TABLE 1 | Chemical composition of the raw materials.

%	SiO_2	MgO	Al_2O_3	CaO	Fe_2O_3	K_2O	Na_2O	P_2O_5	SO_3	Others
SF	94.9	1.1	0.3	0.8	0.2	1.6	0.3	0.4	0.4	0.08
MgO	—	98.5	—	0.02	< 0.01	< 0.01	0.05	< 0.01	0.02	1.85

(Maruyama et al., 2014; Li et al., 2020a). Various studies show that the system has many excellent properties, such as excellent adsorptive properties, especially for heavy metal ions like Cu, Ni (Jia et al., 2016). The M-S-H has a similar structure with sepiolite: it has a large specific surface area and there are unique nano-scale pores in molecular structure, and it has the ability to adsorb heavy metals (Ji et al., 2014; Jia et al., 2017b; Jia et al., 2019; Liu et al., 2021). Magnesium silicate hydrate (M-S-H) phases can be considered as a potential cementitious material for nuclear waste immobilization (Walling et al., 2015) owing to its moderate pH value (varying from ~9.5 to ~10.5) and the Radionuclide (Cs, Sr) sorption potential (Li et al., 2014; Zhang et al., 2020).

The interface region between cement-based material and clay can be observed in the generation of M-S-H, the main components of clay are SiO_2 and Al_2O_3 (Bonen and Cohen, 1992; Santhanam et al., 2020). This study aims to understand the influence of Al^{3+} content on the phase transformation and the structural change of M-S-H. However, the impact of Al^{3+} on the reaction processes during the hydration of M-S-H is poorly investigated. On the contrary, in the presence of Al^{3+}, the molecular structure of C-S-H will change (Song et al., 2021). According to Richardson et al.(Richardson, 1999) the incorporation of aluminium ions (Al^{3+}) could change the molecular structure of the C-S-H phase. For example, tetrahedrally coordinated Al^{3+} [Al (Bernard et al., 2019), Al for tetra-coordination] can substitute for silicon sites in the structure of tobermorite, occupying the bridging tetrahedra sites of C-S-H chains (Bernard et al., 2020; Li et al., 2020b). Magnesium silicate hydrate is formed by reacting MgO with silica fume (SF) and MgO dissolved in water, with one part disassociating with Mg^{2+} and the other part hydrated with water to form $Mg(OH)_2$, and at the same time the SiO_2 dissociates in water to form $H_2SiO_4^{2-}$, and finally the $Mg(OH)_2$, SiO_2, and $H_2SiO_4^{2-}$ react to form M-S-H (Li et al., 2014; Tang and Chen, 2020). The MgO dissolves slowly in water and forms a poorly soluble weak electrolyte, and the $Mg(OH)_2$ is incomplete, which leads to a decrease in the hydration rate of M-S-H (Bernard et al., 2017). The hydration rate of M-S-H can be increased by adding Al^{3+} and thereby can increase the early strength of M-S-H (Li et al., 2019). The M-S-H hydration product was prepared by mixing the reactive MgO, silica fume (SF) and $Al(NO_3)_3$, and the synthesized solids were characterized after 300 days. Advanced testing methods were used to characterize the M-S-H phases prepared under different Al^{3+} contents.

MATERIALS AND METHODS

Materials

Light burned technical grade MgO (Martin Marietta Magnesia Specialties, United States) and SF (Elkem, China) were used to synthesize M-S-H phase. Aluminium nitrate ($Al(NO_3)_3$, (Chempur, China) was used as the aluminium salt. The chemical composition data of the raw materials as reported by the manufacturers are presented in **Table 1**. The median particle sizes of the MgO and silica fume were 3.5 and 0.5 μm respectively.

TABLE 2 | Mix proportion.

Sample ID	Mg:Si(molar ratio)	SiO_2(g)	Al:Si(molar ratio)	w/c
AMSH-1	1:1	6.0	0.01:1	10
AMSH-2	1:1	6.0	0.02:1	10
AMSH-3	1:1	6.0	0.05:1	10
AMSH-4	1:1	6.0	0.10:1	10
AMSH-5	1:1	6.0	0.20:1	10

Experiment Method and Analytical Techniques

The aluminium magnesium silicate hydrate (AMSH) specimens were prepared by mixing the aqueous solutions of MgO, SF, and $Al(NO_3)_3$ at Mg/Si molar ratio of 1:1 and Al/Si molar ratios of 0.01, 0.02, 0.05, 0.1, and 0.2 were presented in **Table 2**. Complete hydration was obtained by adopting a water/solids (W/S) ratio of 10, where S was the total mass of MgO and SF.

In order to speed up the reaction process and make sure the samples were homogenized, the prepared samples were placed in a horizontal oscillator to oscillate for 7 days, and then the solutions were stored at room temperature (25 ± 1 C) in 250 ml sealed polyethylene bottles for up to 300 days. After 300 days the granular residue was separated by filtration and the collected solids were soaked in absolute ethyl alcohol for 24 h to inhibit further hydration, and then dried at 40°C for 48 h. The specimens were characterized using multiple techniques, such as X-ray diffraction analysis (XRD D/Max 2400 V diffractometer with Cu Kα radiation at a scan rate of 0.5 2θ min^{-1}), thermo-gravimetric and derivative thermo-gravimetric analysis (TGA/DTG, alumina crucibles were used and sample were heated in a nitrogen atmosphere between 50°C and 1,000°C at 10°C/min), and field emission scanning electron microscopy (F-SEM: NOVA Nano-SEM 450) on gold coated samples that had been sputter coated for 2 min using 15 mA and 30 Pa pressure and $^{29}Si/^{27}Al$ nuclear magnetic resonance spectroscopy (NMR).

RESULTS AND DISCUSSION

Figure 1 shows the phases transformation in the $MgO\text{-}SiO_2\text{-}H_2O$ system with different Al^{3+} content curing for 1 day and 300 days.

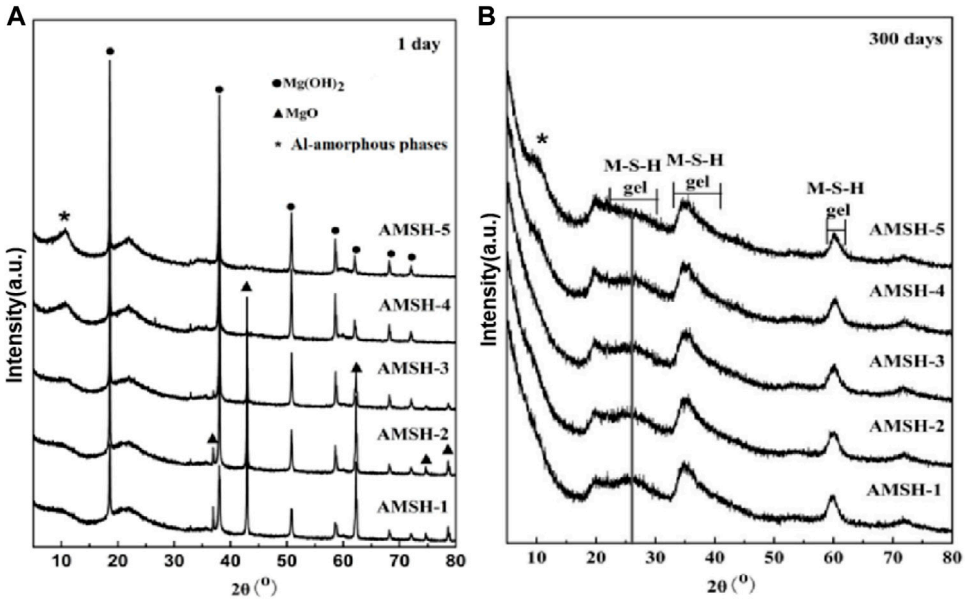

FIGURE 1 | The XRD patterns of magnesium silicate hydrate (M-S-H) samples with different Al^{3+} contents after curing for **(A)** 1 day and **(B)** 300 days.

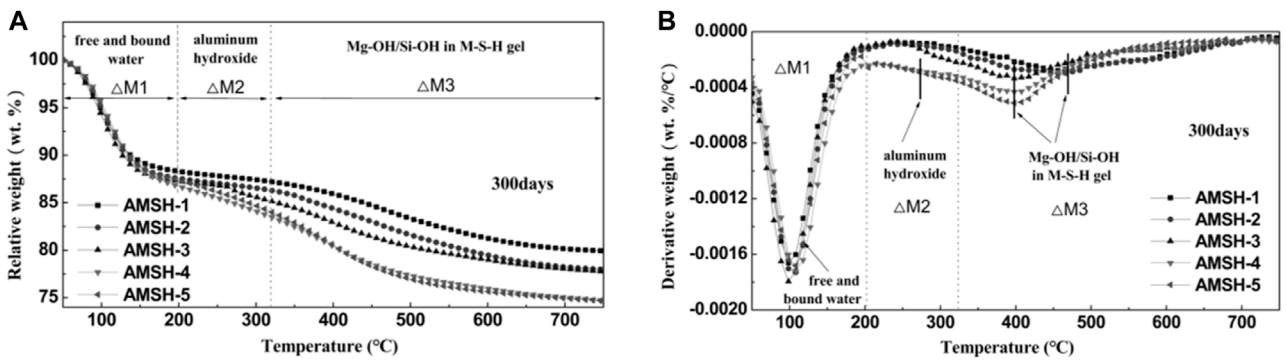

FIGURE 2 | (A) Thermo-gravimetric (TG) and **(B)** Derivative thermo-gravimetric (DTG) data for MSH samples with different Al^{3+} contents after curing for 300 days.

Curing for 1 day it is obvious that with the increase of the dosage of Al $(NO_3)_3$, the content of residual MgO in the system decreases greatly, while the content of Mg $(OH)_2$ increases gradually, which indicates that the addition of Al^{3+} promotes the hydration of MgO and the formation of Mg $(OH)_2$ (**Figure 1A**). At the same time, a dispersion peak appears around 2θ about ~10.6° and it is gradually obvious with the increase of Al^{3+} content, it indicates that there was the formation of a new phase and amorphous type of micro-crystalline hydroxy aluminium. By the later stage of hydration (300 days), the crystalline phases were completely transformed to the amorphous phases due to the reaction of MgO and Mg $(OH)_2$ with silica fume (SF) (**Figure 1B**). The cementitious system is all amorphous phase; and the characteristic peak of M-S-H gel at the broad diffraction at 22–30° becomes weaker with the increase of the dosage of Al^{3+}, which may be the result of the change of molecular structure. The broad diffraction at 20–28°, 33–40° and 58–62° ranges are attributable to the M-S-H phases (Zhang et al., 2014; Jia et al., 2016) (**Figure 1B**) while the diffraction peak between 8° and 12° represents the Al-amorphous phases (**Figures 1A,B**).

Three weight loss stages occurred during the curing of M-S-H for 300 days (**Figure 2**). The first weight loss occurred in the temperature range from 50 to 200°C and is attributed to the removal of free/bound water. The second and third weight losses in the 200–320°C and 320–700°C ranges are attributed to the removal of constitutional water in aluminum hydroxide (Al-amorphous phases) and M-S-H phase respectively (Jia et al., 2016; Nied et al., 2016) (**Figure 2A**). As the dosage of Al^{3+} increases, the weight loss of the phase in the cementitious system increases gradually in the weight loss range of 200°C–400°C, and the weight loss phase in this range may be amorphous or microcrystalline hydroxyl aluminum. According to the weight

TABLE 3 | Mass percents of various components in AMSH samples after curing for 300 days.

	(wt.%)	Free and bound water	$Mg(OH)_2$ (Mg-OH)	gel (Al-OH/Si-OH/Mg-OH)
		ΔM1	ΔM2	ΔM3
300 days	AMSH-1	12.85	—	7.49
	AMSH-2	13.08	—	7.22
	AMSH-3	13.90	—	8.32
	AMSH-4	12.37	—	10.22
	AMSH-5	11.81	—	13.95

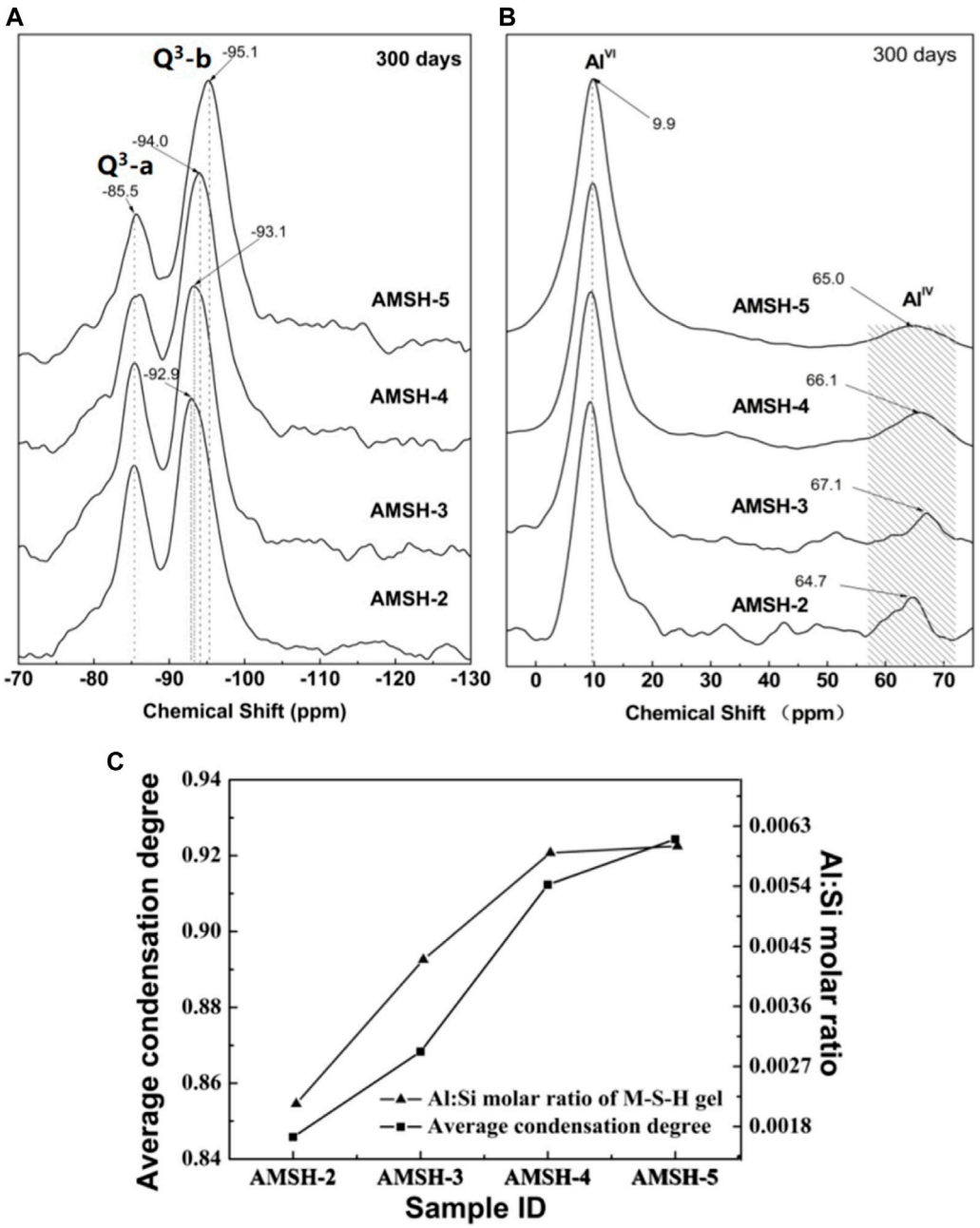

FIGURE 3 | ^{29}Si NMR chemical shifts of MSH samples with different Al^{3+} contents after curing for 300 days **(A)** silica **(B)** aluminum **(C)** changes of the average condensation degree.

TABLE 4 | ^{29}Si NMR chemical shifts (ppm) and relative intensities (%) from de-convolution of the ^{29}Si/^{27}Al NMR spectra for the AMSH-2 ~ 5 samples after curing for 300 days.

Sample ID	Q^1		Q^2		Q^3		Al^{VI}		Al^{IV}	
	Center (ppm)	Area (%)	Center (ppm)	Area (%)	Center (ppm)	Area (%)	Center (ppm)	Area (%)	Center (ppm)	Area (%)
AMSH-2	−79.6 (p)	10.8	−85.3 (p)	24.7	−92.9 (p/Q^3-a)	64.6	9.3 (p)	89.3	64.4 (p)	10.7
AMSH-3	−79.2 (p)	5.8	−85.3 (p)	27.9	−93.1 (p/Q^3-a)	66.3	9.7 (p)	91.4	67.0 (p)	8.6
AMSH-4	−80.2 (p)	4.6	−85.5 (p)	17.1	−94.0 (p/Q^3-a)	78.3	9.9 (p)	94.1	66.0 (p)	5.9
AMSH-5	−78.3 (p)	2.3	−85.5 (p)	18.1	−95.1 (p/Q^3-a)	79.6	9.9 (p)	97.0	65.0 (p)	3.0

Key: p—peak, sh—shoulder, Q^1—Q^1(3OH), Q^2—Q^2(2OH), Q^3-a—Q^3(OH) as continuous layer silicates, Q^3-b—Q^3(OH) as inverted silicates, Q^3-SF—Q^3(OH) in SF.

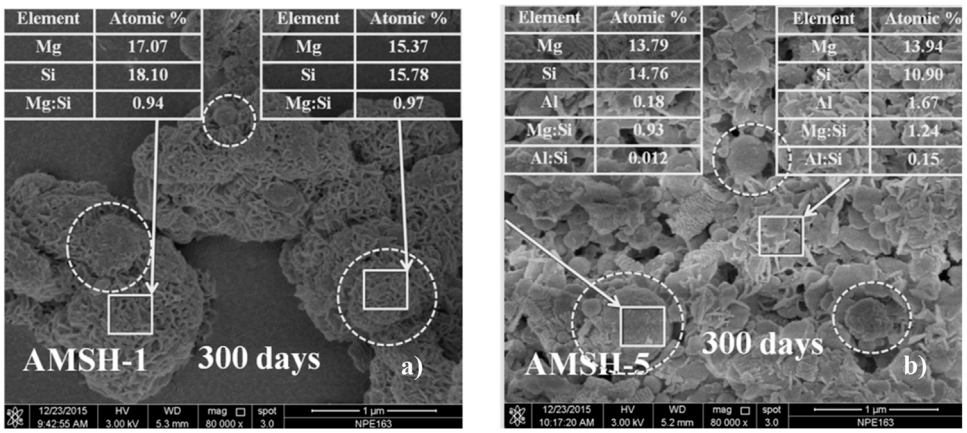

FIGURE 4 | Field emission scanning electron microscope (F-SEM) images of samples with different Al/Si molar ratios after curing for 300 days: **(A)** 0 and **(B)** 0.2.

loss data, the contents of free water and bound water in different samples are basically consistent, indicating that the addition of Al^{3+} did not affect the generation of M-S-H gel when the curing age is long enough and the initial ratio of Al/Si is less than 0.20. As the mass of free and bonding water depends on the porous channel in the MgO-SiO_2-H_2O system but not on the aluminium incorporated, the original structure of the M-S-H phase was unaffected by the incorporated aluminium (**Figure 2B**). The mass percents of various components in AMSH samples after curing for 300 days were shown in **Table 3**.

The molecular structure of the solid solution which included aluminum-amorphous phases (hydroxyl-aluminum) and M-S-H phases was characterized using the NMR. The coordination of the spectrum of ^{29}Si NMR is usually expressed by Q^n, where n represents the bridge oxygen number between each silicon-oxygen tetrahedral unit and other Si atoms. The chemical migration of ^{29}Si in silicate minerals ranges from -60 to -120 ppm and according to different coordination, it can be divided into the following four intervals: -60 to -70 ppm represents a single free island silicate (Q^0); -70 to -83 ppm represents the endpoint of *p*-silicate or chain silicate (Q^1); -83 to -90 ppm represents the silicon-oxygen tetrahedron in the chain silicate (Q^2); -90 to -100 ppm represents the silicon-oxygen tetrahedron in the chain silicate (Q^3); -100 to -120 ppm represents the silicon-oxygen tetrahedron in the three-dimensional reticular silicate (Q^4) (Wei et al., 2006; Wei et al., 2011). The transformation of the microstructure of the M-S-H phase is indicated by the peaks at -85.5 ppm (Q^3-a) and -92.9 to -95.1 ppm (Q^3-b) (**Figure 3A**). In **Figure 3A**, Q^3-a indicates the Si unit via inverted Si-O-Si linkages, while Q^3-b reflects the Si unit in the Si-O tetrahedral layer (Tonelli et al., 2016). **Figure 3B** shows that the coordination of a few Al^{3+} that entered the structure of the M-S-H phase and changed to the tetrahedral coordination [Al (Bernard et al., 2019)]. The chemical shift from -92.9 to -95.1 ppm suggests that Al^{3+} only occupied the Q^3-b tetrahedra sites of the M-S-H layers and did not substitute for the Si^{4+} *via* inverted Si-O-Si linkages (Q^3-a). Although the initial structure of the M-S-H phases was remained unchanged the average condensation degree was increased from 0.84 to 0.92 after the incorporation of Al^{3+} (**Figure 3C**).

Using the deconvolution technique to fit the data of the NMR Test curve, we can figure out the percentage of Si and Al with different coordinations, and the specific data are shown in **Table 4**. After curing for 300 days, the polymerization average degree of M-S-H and Al/Si molar ratio (M (Al: Si)) in M-S-H can be computed by **formula 1** and **formula 2**.

$$CD = (3I(Q3-b) + 3I(Q3-a) + 2I(Q2) + I(Q1)) \times /3(I(Q3-b) + I(Q3-a) + I(Q2) + I(Q1)) \quad (1)$$

$$M(Al{:}\ Si) = n \times I\left(Al^{IV}\right) \quad (2)$$

Where n is the initial Al/Si molar ratio in M-S-H, $I(Al^{IV})$ is the percentage of moles of tetrahedral-Al.

According to **Figure 3C**, with the increase of Al^{3+} incorporation, the polymerization average degree of M-S-H increase from 0.85 to 0.93, but obviously the adding amount of Al^{3+} is still low. When the initial Al/Si molar ratio exceeds 0.1, both the adding amount of Al^{3+} and the polymerization average degree of M-S-H remain at a constant value. The adding of Al^{3+} plays a filling role, as it connects the silicon oxygen tetrahedron chains together and increases the degree of polymerization of the stratified structure. The molecular structure of M-S-H was already highly aggregated, which limits the adding amount of Al^{3+}. It also shows that the number of Si sites in the silicon oxygen tetrahedral chain replaced by Al^{3+} is not large, and that the main function is to connect.

The F-SEM data show that the M-S-H phase has honeycomb morphology and grown on the surface of the SF particles extending to the gaps (**Figure 4A**). The Mg/Si molar ratio of pure M-S-H phases was 0.95. After the incorporation of Al^{3+}, the Mg/Si molar ratio remained unchanged in the M-S-H phases grown on the surface of SF particles, however, increased to 1.24 in M-S-H phases grown in the gaps (**Figures 4A,B**). After curing for 300 days, samples AMSH-1 and AMSH-5 both A and B had only amorphous specimens. The amorphous substance in sample AMSH-1 was still M-S-H gel with villous shape, the villi size was about 10–20 nm and there were a lot of nano-scale pores between the villi. Aluminium incorporation changed the morphology of M-S-H phases from honeycomb to petaline shape (**Figure 4B**).

CONCLUSION

The hydration process of MgO in the magnesium silicate hydrate system was accelerated by the addition of Al^{3+}, and the rate of conversion from MgO to $Mg(OH)_2$ increases with the increase of Al^{3+} content. However, it does not influence the formation of hydration products (M-S-H phases) and it slows down the M-S-H generation. According to TGA/DTG we know that $Mg(OH)_2$ crystals with amorphous hydroxy aluminum are mixed together, which led to the position of weight loss peak being offset, and the increase of the weight loss range from 200°C to 300°C proved that there is a new phase formation in the M-S-H.

Irrespective of the amount of Al^{3+} doped, a limited amount of Al^{3+} entered the structure of the M-S-H phase, consequently, the initial molecular structure of the M-S-H remained unchanged. Aluminium ions occupied the Q^3-b tetrahedra sites of the M-S-H layers and did not substitute for Si^{4+} via inverted Si-O-Si linkages (Q^3-a). The average condensation degree and the Mg:Si molar ratio of the M-S-H phase raised with the increase of Al^{3+} content. Hydroxyl-aluminum, a residual aluminium amorphous phase, and the M-S-H phases formed a solid solution. The addition of Al^{3+} morphology of the M-S-H phase from honeycomb-like to petal-like.

DATA AVAILABILITY STATEMENT

The original contributions presented in the study are included in the article/Supplementary Material, further inquiries can be directed to the corresponding author.

AUTHOR CONTRIBUTIONS

YJ: Conception and design of study. YZ and XZ: Drafting the manuscript. YJ and FL: analysis and/or interpretation of data. WM, HY and RH: revising the manuscript critically for important intellectual content.

FUNDING

This work was supported by the National Natural Science Foundation of China (Grant No. 51808217), the Natural Science Foundation of Hebei Province (Grant No. E2019209403), the S and T Program of Hebei Province (Grant No. 19273803D), and the Research Project of Hebei Province (Grant No. B2019003028).

REFERENCES

Bernard, E., Lothenbach, B., Cau-Dit-Coumes, C., Pochard, I., and Rentsch, D. (2020). Aluminum Incorporation into Magnesium Silicate Hydrate (M-S-H). *Cement concrete Res.* 128, 105931. doi:10.1016/j.cemconres.2019.105931

Bernard, E., Lothenbach, B., Chlique, C., Wyrzykowski, M., Dauzères, A., Pochard, I., et al. (2019). Characterization of Magnesium Silicate Hydrate (M-S-H). *Cement concrete Res.* 116, 309–330. doi:10.1016/j.cemconres.2018.09.007

Bernard, E., Lothenbach, B., Rentsch, D., Pochard, I., and Dauzères, A. (2017). Formation of Magnesium Silicate Hydrates (M-S-H). *Phys. Chem. Earth, Parts A/B/C* 99, 142–157. doi:10.1016/j.pce.2017.02.005

Bonen, D., and Cohen, M. D. (1992). Magnesium Sulfate Attack on portland Cement Paste - II. Chemical and Mineralogical Analyses. *Cement Concrete Res.* 22, 707–718. doi:10.1016/0008-8846(92)90023-o

Ji, X. Y., Guan, W., and Pei, L. (2014). Effect of Polyethylene Glycol Modification on Microstructure and Solubility of Hydrated Calcium Silicate. *J. Funct. Mater.* 45 (1), 1089–1094. doi:10.3969/j.issn.1001-9731.2014.01.020

Jia, S. B., Zhang, X. X., and Li, Y. Y. (2019). Experimental Study on Strength and Leaching Characteristics of Alkali Activated Cement Stabilized Heavy Metal Contaminated Soil. *Ind. Construction* 49 (08), 142–146. doi:10.13204/j.gyjz201908023

Jia, Y., Wang, B. M., Wu, Z. L., and Zhang, T. T. (2017). Effect of CaO on the Reaction Process of MgO-SiO_2-H_2o Cement Pastes. *Mater. Lett.* 192, 48–51. doi:10.1016/j.matlet.2017.01.072

Jia, Y., Wang, B. M., and Zhang, T. T. (2017). *Study on Reaction Mechanism of MgO-SiO2-H2o Cementing System under the Action of NA-HMP and CaO*. Dalian: Dalian University of Technology.

Jia, Y., Wang, B., Wu, Z., Han, J., Zhang, T., Vandeperre, L. J., et al. (2016). Role of Sodium Hexametaphosphate in MgO/SiO2 Cement Pastes. *Cement concrete Res.* 89, 63–71. doi:10.1016/j.cemconres.2016.08.003

Li, J., Geng, G., Myers, R., Yu, Y.-S., Shapiro, D., Carraro, C., et al. (2019). The Chemistry and Structure of Calcium (Alumino) Silicate Hydrate: A Study by XANES, Ptychographic Imaging, and Wide- and Small-Angle Scattering. *Cement Concrete Res.* 115, 367–378. doi:10.1016/j.cemconres.2018.09.008

Li, J., Zhang, W., Garbev, K., Beuchle, G., and Monteiro, P. J. M. (2020). Influences of Cross-Linking and Al Incorporation on the Intrinsic Mechanical Properties

of Tobermorite. *Cement Concrete Res.* 136, 106170. doi:10.1016/j.cemconres.2020.106170

Li, J., Zhang, W., and Monteiro, P. J. M. (2020). Structure and Intrinsic Mechanical Properties of Nanocrystalline Calcium Silicate Hydrate. *ACS Sustain. Chem. Eng.* 8, 12453–12461. doi:10.1021/acssuschemeng.0c03230

Li, Z. H., Zhang, T. S., Hu, J., Tang, Y., Niu, Y. F., Wei, J. X., et al. (2014). Characterization of Reaction Products and Reaction Process of MgO-SiO_2-H_2o System at Room Temperature. *Construction Building Mater.* 61, 252–259. doi:10.1016/j.conbuildmat.2014.03.004

Liu, Y., Mao, Z., Y., Wang, Z., Y., He, Y., Yu, J., and Zhu, Y. (2021). Study on Preparation and Adsorption Properties of Dopamine Modified Sepiolite. *Speciality Petrochemicals* 38 (02), 50–56. doi:10.3969/j.issn.1003-9384.2021.02.010

Lothenbach, B., Nied, D., L'Hôpital, E., Achiedo, G., and Dauzères, A. (2015). Magnesium and Calcium Silicate Hydrates. *Cement concrete Res.* 77, 60–68. doi:10.1016/j.cemconres.2015.06.007

Maruyama, I., Nishioka, Y., Igarashi, G., and Matsui, K. (2014). Microstructural and Bulk Property Changes in Hardened Cement Paste during the First Drying Process. *Cement concrete Res.* 58, 20–34. doi:10.1016/j.cemconres.2014.01.007

Nied, D., Enemark-Rasmussen, K., L'Hopital, E., Skibsted, J., and Lothenbach, B. (2016). Properties of Magnesium Silicate Hydrates (M-S-H). *Cement concrete Res.* 79, 323–332. doi:10.1016/j.cemconres.2015.10.003

Richardson, I. G. (1999). The Nature of C-S-H in Hardened Cements. *Cement concrete Res.* 29, 1131–1147. doi:10.1016/s0008-8846(99)00168-4

Santhanam, M., Cohen, M. D., and Olek, J. (2020). Mechanism of Sulfate Attack: a Fresh Look: Part 1: Summary of Experimental Results. *Cement concrete Res.* 32, 915–921. doi:10.1016/s0008-8846(02)00724-x

Song, Q., Nie, J., Wu, D., Hu, Y. R., and Chen, Y. X. (2021). Effect of SO_4^{2-}, Cl^- and Mg^{2+} on the System of C-S-H and $Ca(OH)_2$. *Construction Building Mater.* 285, 122955. doi:10.1016/j.conbuildmat.2021.122955

Tang, Y., and Chen, W. (2020). Effect of Magnesium on the Structure and Chemical Composition of Calcium Silicate Hydrate at Elevated Temperature. *Construction Building Mater.* 240 (C), 117925. doi:10.1016/j.conbuildmat.2019.117925

Tonelli, M., Martini, F., Calucci, L., Fratini, E., Geppi, M., Ridi, F., et al. (2016). Structural Characterization of Magnesium Silicate Hydrate: towards the Design of Eco-Sustainable Cements. *Dalton Trans.* 45, 3294–3304. doi:10.1039/c5dt03545g

Walling, S. A., Kinoshita, H., BernalCollier, S. A. N. C., Collier, N. C., and Provis, J. L. (2015). Structure and Properties of Binder Gels Formed in the System $Mg(OH)_2$-SiO_2-H_2O for Immobilization of Magnox Sludge. *Dalton Trans.* 44, 8126–8137. doi:10.1039/c5dt00877h

Wei, J. X., Chen, Y., and Li, Y. (2006). The Reaction Mechanism between MgO and Microsilica at Room Temperature. *J. Wuhan Univ. Technology-MaterialsÃ Sci.* 21 (2), 88–91. doi:10.1007/bf02840848

Wei, J. X., Yu, Q. J., Zhang, W. S., and Zhang, H. T. (2011). Reaction Products of MgO and Microsilica Cementitious Materials at Different Temperatures. *J. Wuhan Univ. Technology-Materials Sci.* 4 (26), 745–748. doi:10.1007/s11595-011-0304-3

Zhang, T., Li, T., Zou, J., Li, Y., Zhi, S., Jia, Y., et al. (2020). Immobilization of Radionuclide ^{133}Cs by Magnesium Silicate Hydrate Cement. *Materials (Basel)* 13, 1–17. doi:10.3390/ma13010146

Zhang, T., Vandeperre, L. J., and Cheeseman, C. R. (2014). Formation of Magnesium Silicate Hydrate (M-S-H) Cement Pastes Using Sodium Hexametaphosphate. *Cement concrete Res.* 65, 8–14. doi:10.1016/j.cemconres.2014.07.001

Conflict of Interest: HY and RH was employed by China Railway 14th Bureau Group 2nd Engineering Co., Ltd.

The remaining authors declare that the research was conducted in the absence of any commercial or financial relationships that could be construed as a potential conflict of interest.

Publisher's Note: All claims expressed in this article are solely those of the authors and do not necessarily represent those of their affiliated organizations, or those of the publisher, the editors and the reviewers. Any product that may be evaluated in this article, or claim that may be made by its manufacturer, is not guaranteed or endorsed by the publisher.